Design and Stress Analysis of Quad-Dominated Planar Structures

A Major Qualifying Project (MQP) Report
Submitted to the Faculty of
WORCESTER POLYTECHNIC INSTITUTE
In partial fulfillment of the requirements
For the Degree of Bachelor of Science in

Mechanical Engineering

By:

Samuel Leonard

Project Advisors:

Professor Lee Moradi

Professor Zhikun Hou

Date: April 2022

Abstract

This project implements the mathematical algorithm of generating the ideal parameters for complex glass dome structures. It generates these structures using graph theory and takes the resultant two-dimensional pattern and lifts it to three dimensions. This will ensure that the dome is comprised of plane elements, allowing for the faces of the dome to consist of windows without any warping or bending of glass.

The structure is analyzed using the finite element methods to calculate displacements, forces, and other pertinent parameters for proper selection of material. Safety factors are calculated to show the structural integrity of the dome. The design that is the cheapest to produce while meeting the safety requirements is chosen as the optimal structure.

Acknowledgements

I would like to thank Georgina Quinn, Professor Brigitte Servatius, and Professor Hermann Servatius for working closely with me to develop the understanding required as well as the expansion of the work on the mathematical side of this project. Additionally, I would like to thank Dr. Adriana Hera for her time given to guide me through ANSYS and thoroughly answer my questions. Finally, I would like to thank Professors Lee Moradi and Hou Zhikun for overseeing my project, helping me to find direction and pushing me to get meaningful results every step of the way.

Table of Contents

1.0 Background and Introduction

Truss structures have many applications in modern day society. By generating a simple skeleton of rod elements, shelters, vehicles, cages, and more can be created. One application of such a structure is with domes and skylights. These structures consist of multiple, load-bearing metal rods that support numerous glass panes.

For most metal and glass structures, a very basic geometric pattern is used. These structures consist of triangular sub-elements, allowing for a robust structural system that can withstand environmental forces. There is also a greater ease of manufacturing, as every sub-element will be guaranteed to exist on a plane, eliminating the need to bend or warp glass to fit on the truss structure. William Baker, an architect who gave a talk at the Fields Institute, raised the possibility of using a more complex design consisting of mostly quadrilaterals instead [1]. This requires more complex mathematics to ensure the planarity of each sub-element as well as ensuring the structural integrity of new designs. The benefits of such a quad-dominated design consist of a more aesthetically pleasing structure as well as artistic freedom.

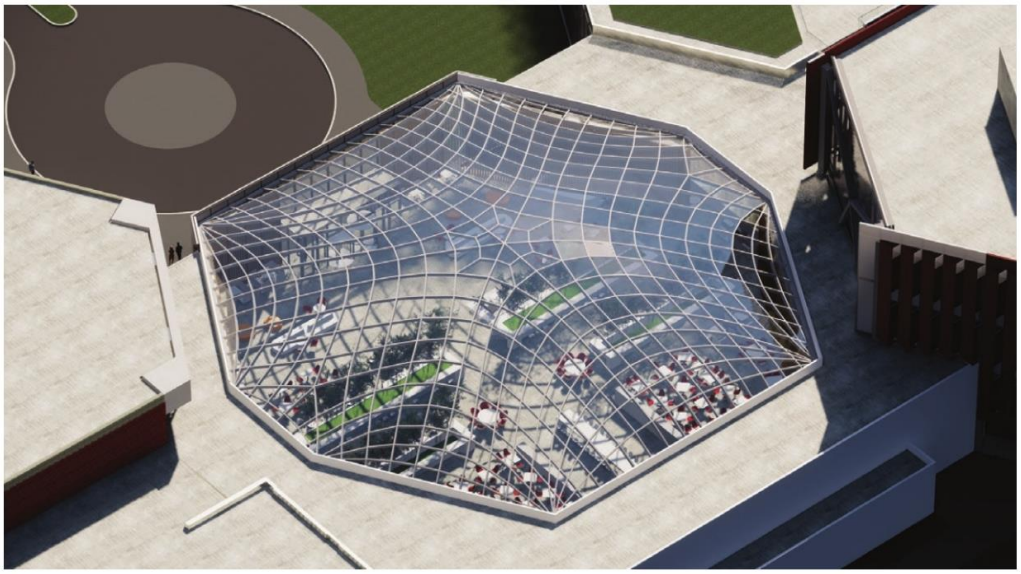

Figure 1: An example of a quad-dominated glass dome

From a purely mathematical perspective, the only constraints are those given by the boundary of the dome as well as the necessity for each face in the framework to be a plane. For a large dome as shown in Figure 1, the boundary conditions would often lie on a flat plane. A two-dimensional pattern can be easily designed and, after calculating a planar lifting, turned into a three-dimensional structure [2,3].

Once a design is chosen, there are very few factors left to manipulate. Material choice is important for the integrity and cost effectiveness of any structure. There are also two more parameters that can be altered, the first being the trusses' sizes and shapes. This will allow for more robust structures at the cost of more complex designs or additional material. Finally, there

is the ability to change the scale of the height. They are all linked due to planarity but can be scaled to any degree. Varying the height to any extreme scale will compromise the design's structural integrity. By manipulating the scale of the dome's height as well as the truss size, the robustness of the design as well as the cost will be affected. With any potential problem, there is a best design with a set height and truss size; it will be the most economical structure that can withstand the environmental forces imposed.

The goal of this MQP is to better analyze the practicality of generated structures and devise a technique to optimize them with respect to their heights and beam dimensions. The first step will be looking at desired material properties and deciding upon which material(s) are the most economical to use. Next, it will be important to look at building codes and expected forces the structures would have to withstand. Finally, the structure can be analyzed at differing heights and truss parameters to ensure that it will be safe in real-life conditions.

2.0 Mathematical Generation of a Problem

2.1 Requirements and Constraints

For any given project, one must first establish the requirements and constraints. In the case of creating a dome-like skylight, we select: *A large mall constructed with a skylight of approximately 10 meters by 14 meters to allow for sunlight to enter the building.*

2.2 Generating a Two-Dimensional Design

Given the rough shape of the skylight, the next step is to generate a border for the design. The border can be generated as a polygon with any number of edges. However, generating more edges will result in larger material cost and more complexity. One must balance the quantitative factors such as edge count and the consequential amount of material with the qualitative factors such as beauty in complexity. There is some freedom of choice here, however a decagon is a nice shape, as it allows for complex interior patterns without utilizing an excessive amount of interior trusses and driving up material cost. Figure 2.2 below shows such a shape centered on the origin. The larger the degree of the polygon, the more quadrilaterals will be formed in the later steps. If the desired skylight was larger, a more complex shape can be chosen to allow for a more quadrilateral-dominated design.

In order to ensure the design has a planar lift, a specific type of graph within graph theory must be generated. This can be done by using a Hamiltonian cycle within the border, treating each overlapping edge as a new point, and removing two of the edges left. By This ensures the three-dimensional design will be dome-like in structure while every face remains a plane. The process is shown below in Figure 2.2, starting from the border (left) to the interior cycle generated (middle) and its deformation and simplification (right).

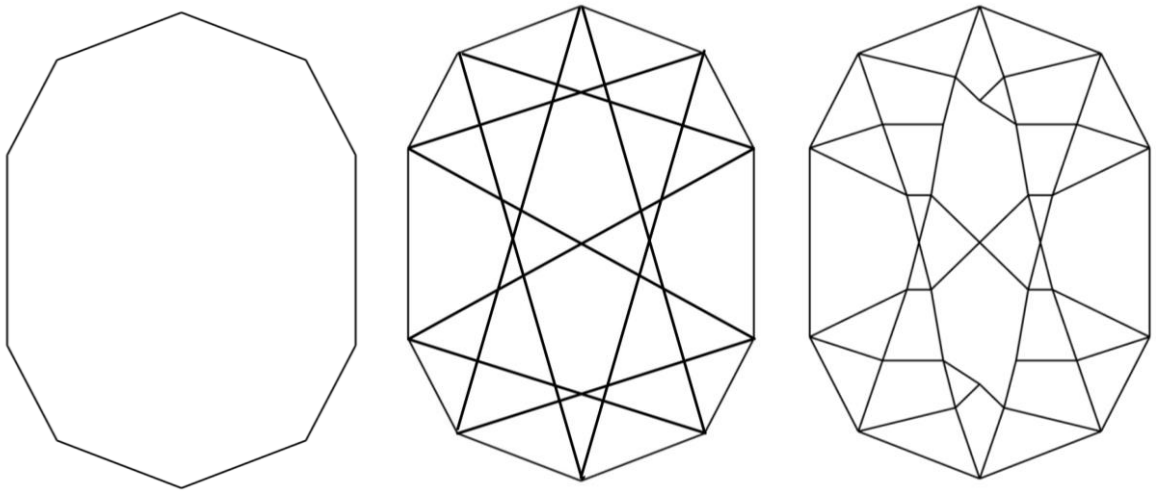

Figure 2.2: The generation of the two-dimensional design of a dome

A variety of shapes can be generated in the middle step; however, some of these shapes can be many-sided polygons, parallel lines, or other geometries which can result in a weaker structure. A set of triangular shapes were generated in as many areas as possible. Where necessary, rectangular shapes were included with the use of beam element in their perimeter. The design was simplified slightly by shifting the intersections of points to allow for aesthetics.

2.3 Calculating Respective Heights of the Dome

Once the two-dimensional graph is finalized, it can be lifted into three dimensions. This is done by calculating the plane equation for each face and then calculating the z-coordinate using the plane equation.

The first step is to calculate proportional forces within the two-dimensional graph. By taking an arbitrary edge and instilling an internal force on it, the rest of the forces can be computed. This self-resolving property is why only specific graphs can be used, requiring the process outlined in section 2.2. A simple example can be shown with a K_4 graph. The edge e_{12} was arbitrarily chosen to have a tension force of 1 Newton in it. Using the method of joints, P_1 can be analyzed and the values for internal forces can be found for e_{13} and e_{14}. This process can be repeated for every single point until all edges have an internal force as shown in Figure 2.3.1.

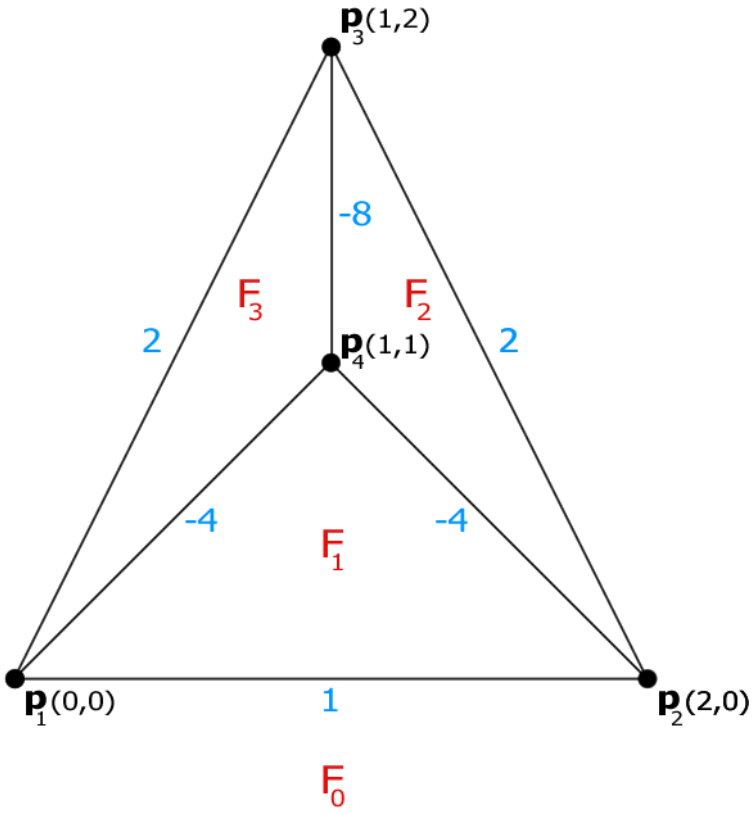

Figure 2.3.1 Labeling and Internal Stresses of a Simple Two-Dimensional Graph

A shortcut for calculating the stresses consists of representing each edge as a constraining linear equation and generating a rigidity matrix from the resultant system of equations. The left null space of this matrix will be a basis for all possible solutions for the edges' internal stresses.

To calculate the liftings, a plane equation for each face of the graph is used. Since any two planes intersect at a single line, we can calculate the equation of adjacent planes using the line crossed as well as a scaling factor found from the internal stresses:

$$F_{k+1} = F_k + \omega_{ij}\,[[p_j - p_i] \times [p_0 - p_i]]_z$$

With any planar equation F_k given, an adjacent plane's equation F_{k+1} can also be found. Here, p_j-p_i represents the edge that borders the two faces. p_0-p_i is an arbitrary crossing of this edge. The self-resolving stress found for each edge is ω_{ij} and is a scaling factor used in the lifting [3].

Since the structure is assumed to be on a flat surface, the equation for the surrounding plane is z = 0. From here, the adjacent planes can have an equation calculated until every plane is solved for. For the K_4 example this can be shown as follows. Note that the labeling convention of points and faces is consistent with Figure 2.3.1:

$$F_1 = F_0 + (1)[[(2,0,0) - (0,0,0)]\ x\ [(x,y,0) - (0,0,0)]]_z$$
$$F_1 = 0 + (1)\,[[(2,0,0)]\ x\ [(x,y,0)]]_z$$
$$F_1 = 0 + (1)(2y)$$
$$F_1 = 2y$$

Every single face can be calculated the same way, giving the following equations for each plane:

$F_0 = 0$ $F_1 = 2y$ $F_2 = -4x-2y+8$ $F_3 = 4x-2y$.

This allows every single plane to be calculated in the graph and a three-dimensional height to be calculated. For example, the one non-border node in the K_4 example exists at the coordinates (1,1). Its height, found using the equation for any of the adjacent planes (F_1,F_2, or F_3) can be calculated to be 2 units.

This method can be done on much more complex shapes, such as the graph from Figure 2.2. By going through these calculations, a model can be generated, as shown in Figure 2.3.2. Here, all 34 faces of the structure are lifted to create planes. This structure is ideal for window-filled domes, as glass is easily produced as planar elements.

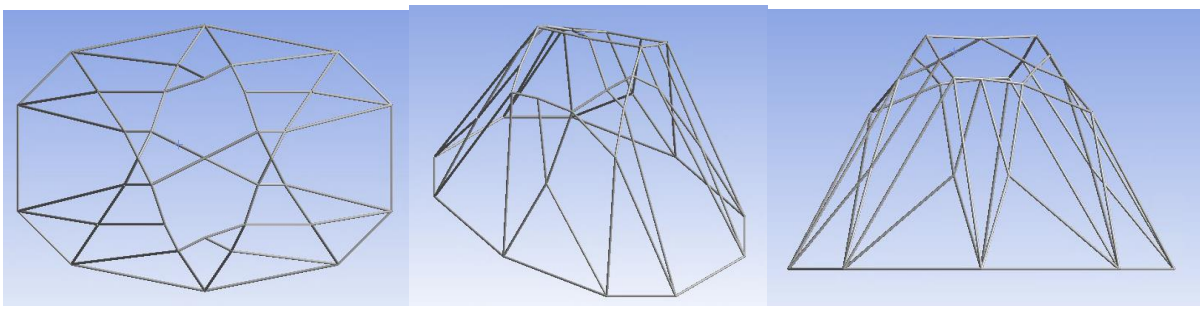

Figure 2.3.2: A 3D Model of the Graph from Figure 3c from different angles

The one degree of freedom in this analysis is the initial, arbitrary force instilled on the graph's edge. It can be any value, and all other values will be proportionally altered. This means that ω_{ij} can be proportionally scaled, which will consequently allow the height to be scaled as well. This is easier to visualize on the K_4 example; the middle point lifted into three-dimensional space creates a triangular pyramid. Scaling this height will still result in a triangular pyramid with planar surfaces. The same is true for Figure 2.3.2: Scaling the height of all the points will result in a structure that still consists of planar surfaces.

3.0 Design of the Dome Structure

3.1 Material Choice

Material choice is important for any structure. The strength and stiffness of the material will determine the entire structure's stability, and the density of the material will affect the weight of the structure. When dealing with a dome-like structure, there are two materials that need to be picked: the material for the trusses and the material for the windows.

3.1.1 Beam Material

Both structural steel and wrought aluminum are most commonly used to build domes, and their properties are shown in Table 3.1.1. The main difference between the two materials is the density, where aluminum is shown to be significantly lighter.

Table 3.1.1: Material Properties of Steel and Aluminum [4]

Material	**Tensile Yield Strength (Pa)**	**Compressive Yield Strength (Pa)**	**Young's Modulus (Pa)**	**Density (kg/m^3)**
Structural Steel	$2.5 * 10^8$	$2.5 * 10^8$	$2 * 10^{11}$	7850
Wrought Aluminum 6061-T6	$2.76 * 10^8$	$2.4 * 10^8$	$6.904 * 10^{10}$	2713

Aluminum is selected due to its lighter density, which results in reduced dead and seismic loads on the structure.

3.1.2 Window Material

The windows are assumed to not be load-bearing, so the only parameters relevant for the analysis are the glass density, thickness, and potential non-structural benefits. The most important non-structural benefit is insulation. The ceiling of any building is where a majority of heat leaves in the winter or enters in the summer, driving up energy costs and carbon footprint of a building. For this reason, it is important that the window is insulated, leading to the choice of a double paned, glazed glass. Additionally, a phase-change material (PCM) layer could be added to greatly reduce heat transfer as described in Liu et al. [5]. This allows for a 6-layer structure, consisting of four 4mm panes of glass, one 12mm layer of PCM and two layers of air. The density and total thickness of these layers are detailed in Table 3.1.2

By prioritizing heat insulation, the upfront cost of the structure will be increased. The greater cost of the windows is compounded by the extra weight, requiring a more robust and costly truss structure. However, this design will reduce maintenance costs significantly over time. Since the overall cost of the insulated design will be cheaper as well as more sustainable, it is chosen over a simple, single-plated glass roof.

Table 3.1.2: Material Properties of Glass and PCM [5]

Material	Total Thickness (m)	Density (kg/m^3)
Glass	0.016	2500
PCM	0.012	890

3.2 Finite Element Modeling with ANSYS

In order to calculate the structural integrity of the dome structure, a static analysis is performed using the ANSYS finite element code. After generating a model, static analysis can be utilized to find displacements, axial forces, and support reactions. Once these results are known, proper aluminum structural shapes are selected, and the structure can be classified as sound [4].

3.2.1 Key Assumptions

Three key assumptions are made during the finite element analysis of the design. The finite element method first involves breaking a structure into numerous elements, and then using the conditions along each element to solve for values such as displacement and stress. The first assumption that needs to be made is the shape of the elements that are being utilized. The more complicated the shape, the more accurate the analysis tends to be, but computation time also grows rapidly with complexity. Since each rod in the structure is traveling along a single, 3-dimensional vector, it can be modeled as either a truss/link structure or as a beam structure. Due to the nature of the incident forces acting as pressures against the structure's elements, it is best to use the beam model which can break the structure down further and measure moments in addition to axial forces. This is an important feature when it comes to distributing the windows' loads accurately onto the aluminum framework.

Another assumption is that the structure's glass windows do not take tension or compression loads. Instead, they will be modeled to only take pressure, instilled by natural forces such as snow and wind. The aluminum trusses are load bearing while the glass panes are attached to them in a way such that the glass does not experience any heavy tension or compression loads. This is a simplification, but forces can be strongly mitigated depending on the method of installation. In this model, the glass windows experience lateral pressures which are directly transferred to the neighboring aluminum trusses.

A final assumption regarding the model has to do with the geometry of the beams. To help simplify calculations as well as improve the aesthetics of the design, each of the beams will be modeled as a cylindrical rod.

3.2.2 Adding Members for Structural Stability

Due to the assumption of non-load bearing faces, the design from Figure 2.3 becomes considerably weaker. To help alleviate this issue, more beams can be added to improve structural integrity and prevent failure. Potential designs were put into the ANSYS software to analyze their integrity. There were numerous potential designs that were stable. After running multiple versions of these designs, the one shown in Figure 3.2.2 had the smallest axial forces under the rod weight alone. Since reducing axial forces was the focus of the design optimization, this design was chosen.

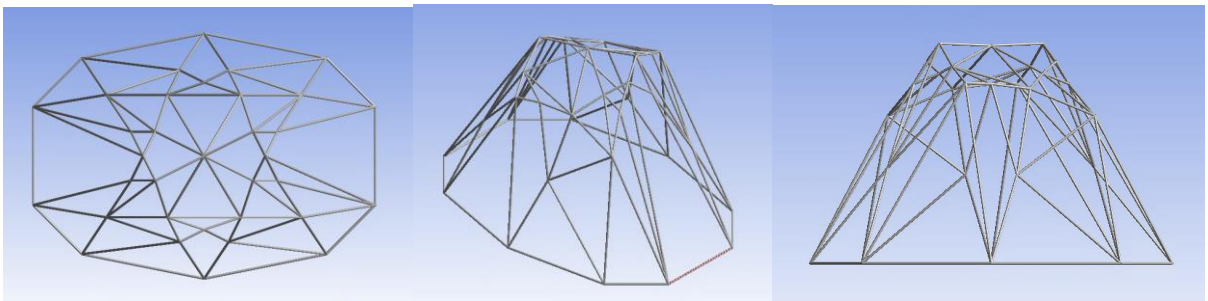

Figure 3.2.2: The 3D Model with additional trusses to allow for analysis and structural integrity

Now that the three-dimensional shape is optimized, the parameters that can still be altered are the truss size and the scale of the height. The variations of these parameters are further laid out in Section 4.2.

3.2.3 Preliminary Analysis of Varying Structure Heights under Gravity

The shape in Figure 3.2.2 can be modified to have different scaled heights. Using the model as the basis, we can look at the initial differences in forces when dealing with heights that are doubled or halved.

Table 3.2.3 Variations of Heights and Resultant Forces/Deformations for 5 cm Radius Beam

Max Height (m)	**4.256**	**8.512**	**17.024**
Max Tension Force (N)	51999	1.04E+05	57451
Min Compressive Force (N)	-53601	-1.07E+05	-51362
Max Deformation (m)	0.14895	0.5958	0.12989

The results show that the deformation and axial forces are at a maximum for the 8.512-meter-tall structure. All these values decrease when the height is either doubled or halved. This is

explained by the fact that a larger height has larger angles, allowing for a lower magnitude of forces due to the interaction between members, while a smaller height has less material and therefore less weight. With less tensile and compressive forces acting on the members, less deformation can be expected.

3.5 External Forces

In real life, a dome-like structure will face many environmental forces. The five main forces that will be taken into consideration are the dead load, live load, wind load, snow load, and earthquake load. Due to the fact that the latter three of these loads are geography dependent, a location for the design must be determined before analysis is possible. This model will be planned for Worcester, Massachusetts to allow for a quantitative analysis of these forces.

3.5.1 Building Codes

To ensure the safety of the design, it is important to look at the building codes. These are well researched, municipal dependent building parameters that tell the expected forces. The values in Table 3.5.1 give information regarding the loads expected from the 3 geography dependent forces in Worcester, Massachusetts.

Table 3.5.1 Snow Loads, Wind Speeds, and Seismic Parameters for Worcester, MA [6]

	Snow Loads		**Basic Wind Speed V_{ult} (mph)**			**Seismic Parameters (%g)**	
City/Town	**Ground Snow Load, P_g (psf)**	**Minimum Flat Roof Snow Load, P_f[1] (psf)**	**Risk Category I**	**Risk Category II**	**Risk Category III or IV**	**S_s**	**S_1**
Worcester, MA	50	35	114	124	134	0.18	0.066

An important observation is the risk categories in the basic wind speed section. According to Table 1604.5: Risk Category of Buildings and Other Structures in the MA State Building Code, our design would have to face regulations for risk category III since our original problem concerned a mall, meaning our building falls under “Any other occupancy with an occupant load greater than 5,000.” [6].

3.5.2 Dead Load

The dead load will consist of the weight of the entire structure. The finite element analysis of the structure will automatically compute the mass of the truss structure given the density and mass of materials.

The dead load can be calculated by hand by finding the mass of the entire structure. Due to varying heights and trusses, the mass can be found in terms of parameters of the structure. First, each truss element's length can be calculated using the distance formula in three-dimensional space.

$$L_i = \sqrt{(x_2 - x_1)^2 + (y_2 - y_1)^2 + (z_2 - z_1)^2}$$

Since each truss member will be modeled as a cylindrical rod, the final value for the dead load is

$$F_{Dead\ Load\ Beams} = mg = V\rho g = \Sigma L_i \pi r^2 \rho g$$

By substituting in the values for the density of aluminum and gravity, a simplified equation is found.

$$F_{Dead\ Load\ Beams} = 83612\ \Sigma L_i r^2$$

The weight of the glass panes will be proportionally distributed to the aluminum elements touching the pane. Due to the way ANSYS computes rigid bodies, this will need to be found independently of the program and then represented as a collection of remote forces acting on the truss structure. Previously, the densities and thicknesses of the window elements were found. These values can be used along with the surface area of each face to calculate the weight.

$$F_{Dead\ Load\ Windows} = mg = V\rho g = \Sigma A_s(t_1\rho_1 + t_2\rho_2)g$$
$$F_{Dead\ Load\ Windows} = \Sigma A_s(0.016 * 2500 + 0.012 * 890)9.81$$
$$F_{Dead\ Load\ Windows} = 497.1708\ \Sigma A_s$$

These values are all calculated in the appendix Table A1. Note that they are calculated independent of the rod radius. This is due to negligible changes, as the differences in areas will be on the order of hundredths and not affect the weight in any significant manner.

3.5.3 Live Load

The live load will consist of any additions to the structure, such as mechanical and electrical equipment, light fixtures, or any other items that may be added to the roof structure after the initial construction phase. For the purpose of this analysis, a live load of 20 pounds per square foot (2394 Pa) will be applied to the entire surface of the dome [7]. Similar to the dead load for the glass windows, this will be calculated by multiplying the load by the area and treating it as a remote force in ANSYS.

$$F_{Live\ Load} = 2394\ \Sigma A_s$$

These values are calculated in Table A1. As with the windows' dead loads, they are independent of the rod radius due to its negligible effects. The effect of the live load on the aluminum beams are also assumed to be negligible.

3.5.4 Wind Load

The wind load on the dome structure will be based on the worst-case scenario winds outlined in the building code of the State of Massachusetts for the city of Worcester. Two variations of the same force are imposed by the wind load. The side of the dome that the wind is directly hitting is called the windward side and it has a windward force imposed on it. The windward force can be calculated using geometry and worst-case scenario wind velocity. The other side of the structure is called the leeward side. The leeward force is calculated as a percentage of the windward force. For this model, the wind will be assumed to be blowing in the positive z direction, as shown in Figure 3.5.4. This direction is one of the largest cross-sectional areas of the model, allowing for the worst-case forces to be analyzed. Once the direction of the wind is set, the windward and leeward forces can be calculated.

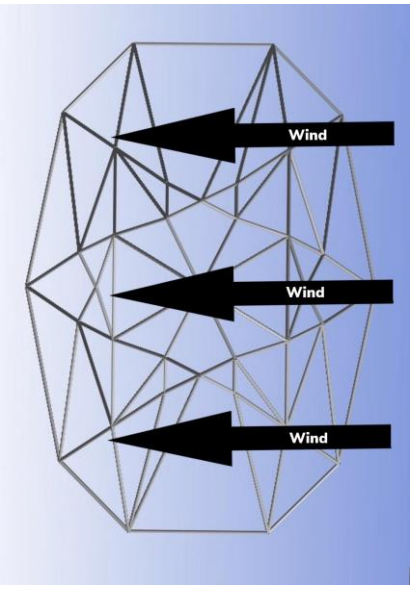

Figure 3.5.4 Direction of Wind Flow

According to Table 1611.8 in the State Board of Building Regulations and Standards, the leeward force can be calculated as half of the windward force [8]. This value applies to standard roofs, and loses some accuracy in this situation due to the dome's nature. To improve the accuracy, the wind force is calculated for each individual pane, and is halved if the face is on the leeward side.

The wind force is equal to the wind pressure multiplied by the affected area. In order to calculate the wind force, the cross sectional area is first calculated, available in Table A2.

Meanwhile, the wind pressure is a function of the wind speed and roof angle [9,10]. The International Institute of Building Enclosure Consultants [9] provides the following equation to find wind pressure in terms of wind speed and coefficient of drag,

$$P = C_d 0.00256 V^2$$

where C_d is the drag coefficient and V is the wind speed in mph. NASA [10] simplifies the equation for C_d in terms of roof angle.

$$C_d \sim 1.28\, sin(\alpha)$$

An approximate angle α has been calculated for every face and is shown in Table A2. These are approximations, as the angles between the sub-elements' planes and the horizontal plane were calculated, rather than the angle of incline relative to the incoming wind. Due to the dome-like structure, very few planes are perfectly in line with the wind, meaning complex equations would be needed to find the pressure, as α changes within any given face. However, this approximation is acceptable, as the values are nearly the same for faces with the largest cross-sectional area, and as potential error in α grows, the value of the cross-sectional area shrinks, meaning the resultant forces are not as significant.

$$P = 1.28\, sin(\alpha) 0.00256 V^2$$

As seen in Table 3.5.1, the wind speed used for this analysis will be 134 mph (59.9 m/s),

$$P = 11.75719\, sin(\alpha)$$

so, the resultant windward load will become

$$F_{Wind\ Windward\ Load} = \Sigma(11.75719\, A_{CS_{Horizontal}}\, sin(\alpha))$$

Since the direction has been fixed, half of the faces are on the leeward side. Their wind forces will be half of the windward load [8].

$$F_{Wind\ Leeward\ Load} = \Sigma(5.87860\, A_{CS_{Horizontal}}\, sin(\alpha))$$

These windward and leeward forces can be found in Table A2 and will be treated as a remote force in ANSYS similar to the other window-based forces. The wind force applied to the aluminum rods is assumed to be negligible.

3.5.5 Snow Load

The snow load on the dome structure will be based on the worst-case scenario snowfall outlined in the building code of the State of Massachusetts for the city of Worcester. This will be calculated in ANSYS using the same methods as the other window-based loads: first the magnitude must be found through calculation and then added into the model as a remote force.

The precipitation load also relies on building codes and the geometry of the structure. The roof snow load depends on three main factors: the area of the roof, the angle of incline it possesses, and the ground snow load. The area of the roof and the angle of incline are used in order to find the projected vertical area of each face. This was calculated independently to avoid rounding errors and the results can be found in Table A3. The ground snow load can be multiplied by the projected vertical area of each face to find each face's roof snow load [11,12].

$$F_{Snow\ Roof\ Load} = \Sigma(A_{CS} cos(\alpha) F_{Snow\ Ground\ Load})$$
$$F_{Snow\ Roof\ Load} = \Sigma(A_{CS_{Vertical}} F_{Snow\ Ground\ Load})$$

The value for $F_{Snow\ Ground\ Load}$ from Table 3.5.1 is 50 psf (2394 Pa). Substituting this value into the above equation gives the following:

$$F_{Snow\ Roof\ Load} = \Sigma(2394\ A_{CS_{Vertical}})$$

3.5.6 Seismic Load

The final load considered is the seismic load, caused by earthquakes. Although the seismic load effects in New England are relatively small, they can still cause structural failure when compiled with other loads. The seismic load will be based on worst-case scenario seismic shifts as recommended by the building code of the State of Massachusetts for the city of Worcester.

Seismic Loads depend on the given values of s_s and s_1. These represent the acceleration of the structure as a percentage of gravity given previous earthquake data, where s_s is the value over short periods and s_1 is the value at a period of 1 second. [13]. When designing for worst-case scenarios, the larger of the two forces should be utilized. For the city of Worcester, this means taking the value of s_s, which is 0.18. This means that there will be some acceleration in the horizontal direction equivalent to 0.18g or 1.77 m/s^2. The direction is arbitrary, but for the maximal damage, it will be aligned with the wind in the positive z direction.

The force for this value can be found by multiplying this acceleration by the mass, similarly to finding the dead loads, just with a horizontal, fractional gravity.

$$F_{Seismic\ load\ beams} = 0.18 * 83612\ \Sigma L_i r^2$$

$$F_{Seismic\ load\ windows} = 0.18 * 497.1708\ \Sigma A_s$$

$$F_{Seismic\ load\ beams} = 15050.16\ \Sigma L_i r^2$$
$$F_{Seismic\ load\ windows} = 89.4907\ \Sigma A_s$$

In ANSYS, the seismic load for the beams can be automatically calculated by inserting a horizontal acceleration of 1.77 m/s^2 that affects all of the beams. This force is the result of their mass times the imposed acceleration. The seismic load for each window will have to be calculated individually and treated as a remote force acting on the face's neighboring beams. These calculations are available in Table A4. It is noted that due to time constraints, seismic load calculations ignored the natural frequencies of the dome and the structure beneath it. This simplification will significantly increase the risk factors in the integrity of the dome structure. Therefore, the results in this report should not be used for any actual construction, rather a demonstration of how to incorporate a seismic load.

4.0 Results

4.1 Failure Force Analysis

When coming up with a final design for the structure, it is important to look at the factors that can cause structural failure. The two main factors for failure are the axial forces and the radii of the truss members. By increasing the radii, the stress levels within each member are decreased; the area is increased greatly and the force values of $F_{\text{Dead Load Beams}}$ and $F_{\text{Seismic Load Beams}}$ are increased, but to a lesser extent. The change in height also affects the axial forces greatly, especially when sharp angles or excessive additions in material are added into the design.

4.1.1 Tensile and Compressive Stresses

Both Tensile and Compressive stresses are computed in Pa, which is the axial force of the truss divided by the cross-sectional area. Table 4.1.1 has the maximum tensile and compressive forces for each instance, as well as the resultant stresses and safety factors. Recall from Table 3.1.1 the tensile and compressive strengths of aluminum in Pa are $2.76*10^8$ and $2.4*10^8$ respectively. The safety factor is the lower of the tensile and compressive safety factors.

Table 4.1.1: Tensile and Compressive Safety Factors

Design Max Height (m)	Beam Radius (m)	Max Tensile Force (N)	Max Compressive Force (N)	Max Tensile Stress (Pa)	Max Compressive Stress (Pa)	Safety Factor
4.256	0.05	40877	-105480	5204621.29	-13430130.72	17.87

4.256	0.075	28732	-98273	1625898.60	-5561114.21	43.16
4.256	0.1	23934	-100390	761842.88	-3195512.95	75.11
4.256	0.125	22186	-108350	451969.48	-2207288.07	108.73
8.512	0.05	52886	-146760	6733654.66	-18686063.56	12.84
8.512	0.075	48240	-164650	2729825.58	-9317284.05	25.76
8.512	0.1	52490	-201690	1670808.59	-6419992.09	37.38
8.512	0.125	63055	-252870	1284545.91	-5151425.34	46.59
17.024	0.05	87115	-221550	11091826.29	-28208622.11	8.51
17.024	0.075	89537	-262850	5066757.74	-14874267.30	16.14
17.024	0.1	107500	-339560	3421831.28	-10808530.50	22.20
17.024	0.125	133680	-443660	2723306.60	-9038167.30	26.55

4.1.2 Buckling

One important mode of structural failure is through the buckling of members under compression. With large compressive loads, a truss element can buckle before reaching its compressive strength. In order to calculate the maximum amount of force that a rod can handle before buckling, the following equation can be used:

$$F_{critical} = n\pi^2 \frac{EI}{L^2}$$

Due to the geometry of the problem, we can simplify this equation further, into recognizable terms. Each truss in the model is portrayed as a rod with a pinned joint on either side, allowing *n* to be equal to one. *I* can also be found using the geometry of a cylinder.

$$I = \frac{1}{4}\pi r^4$$

This simplifies the equation for $F_{critical}$ into terms of radius, length, and material properties.

$$F_{critical} = \pi^3 \frac{Er^4}{4L^2}$$

Note that there are two ways to increase $F_{critical}$ by a factor of k without changing the material. The first would be to reduce L to $\frac{1}{\sqrt{k}}L$. However, there are only two ways to shorten the length: either decrease the height or increase the number of trusses. The other way to increase $F_{critical}$ by k is to increase the radius to $\sqrt[4]{k}\,r$. This will increase the forces present in the structure as well, but only be a factor of $\sqrt{k}$, since they depend on cross-sectional area. In this case, adding this slight amount of more material is more beneficial than reconstructing the entire truss structure to shorten the length. It will increase the cost but adding numerous more members will both increase the cost as well as take away from the aesthetic appeal. Before ensuring the design's validity, each member will be quickly checked for buckling. These values of the critical buckling forces are listed in Table A7. Table 4.1.2 shows the relevant safety factors with respect to buckling forces. These relevant factors are the safety factor of beam 38, as it has one of the longer lengths as well as the largest compressive force.

Table 4.1.2: Buckling Safety Factors

Design Max Height (m)	Beam Radius (m)	Most Likely Beam to Buckle	Beam's Critical Buckling Force (N)	Max Compressive Force (N)	Safety Factor
4.256	0.05	38	500726.07	-105480.00	4.75
4.256	0.075	38	2534925.74	-98273.00	25.79
4.256	0.1	38	8011617.17	-100390.00	79.80
4.256	0.125	38	19559612.22	-108350.00	180.52
8.512	0.05	38	197105.35	-146760.00	1.34
8.512	0.075	38	997845.83	-164650.00	6.06
8.512	0.1	38	3153685.60	-201690.00	15.64
8.512	0.125	38	7699427.72	-252870.00	30.45
17.024	0.05	38	57541.55	-221550.00	0.26
17.024	0.075	38	291304.11	-262850.00	1.11
17.024	0.1	38	920664.85	-339560.00	2.71
17.024	0.125	38	2247716.92	-443660.00	5.07

4.2 Working Designs

Table 4.2.1 shows how each design performed, and whether it failed due to tension, compression, or buckling. Multiple models were run with varying heights and rod radii. The safety factors for tension, compression, and buckling were found and the minimum of the three was recorded as the structure's final safety factor. For aluminum structures, the safety factor should be 1.65 [14]. The structures that did not meet this requirement are marked red in Table 4.2.1.

Table 4.2.1 Varying Design Safety Factors

	0.05m Radius	0.075m Radius	0.1m Radius	0.125m Radius
4.256m Max Height	4.75	25.79	75.11	108.73
8.512m Max Height	1.34	6.06	15.64	30.45
17.024m Max Height	0.26	1.11	2.71	5.07

Another design consideration is the maximum deflection. Table 4.2.2 has the values of the max deflections. This happened in all models on a truss of lengths 5.39m, 8.08m or 14.49m, varying with the maximum heights of 4.256m, 8.512m, and 17.024m respectively. The most exaggerated example of this is shown below in Figure 4.2

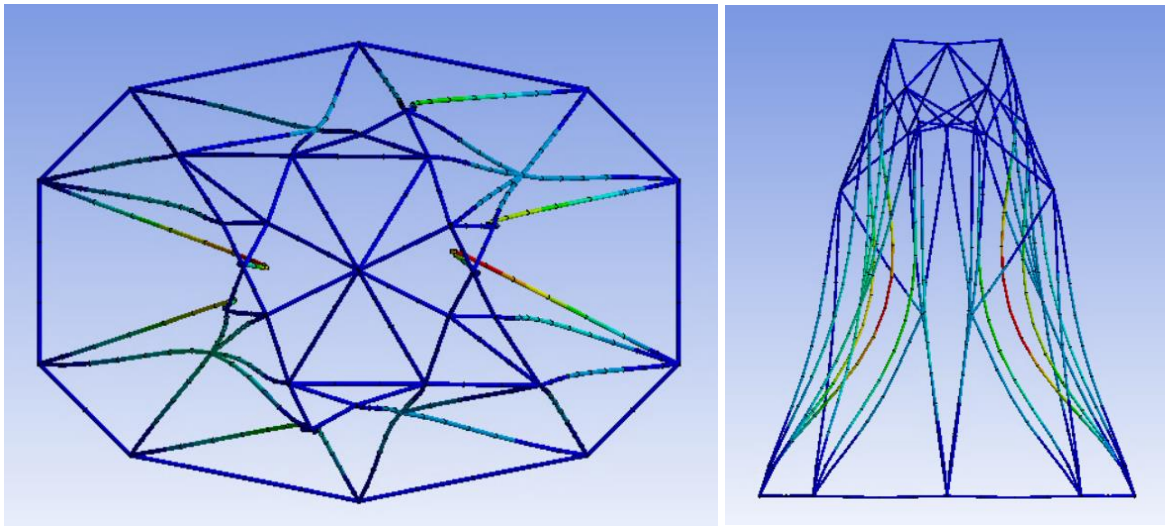

Figure 4.2: The Deflection of the Structure with a Max Height of 17.024m and Rod Radius of 0.05m (Exaggerated by fourteen times the true deformation)

Aluminum structures should not have a deflection of more than 1/60th of the length [15]. This means that the respective maximum deflections are 0.0898m for the structure with the max height of 4.256m, 0.1347m for the structure with a max height of 8.512m, and 0.2415m for the

structure with a max height of 17.024m. The deflections that are greater than these conditions are marked in red in Table 4.3.2.

Table 4.2.2: Max Deflections

	0.05m Radius	0.075m Radius	0.1m Radius	0.125m Radius
4.256m Max Height	0.377m	0.0083m	0.0030m	0.0014m
8.512m Max Height	0.0408m	0.0101m	0.0042m	0.0022m
17.024m Max Height	0.2036m	0.0593m	0.0228m	0.0128m

Table 4.2.3 shows the amount of material for each of the working models and estimates the cost as a result. This is the combined costs based on the weight of the metal and the surface area of the glass, where it is estimated to be $1.3846 per pound of aluminum [16] and $200 per square meter of glass [17]. The optimal result would be the one that is both safe and lowest in cost.

Table 4.2.3 Approximate Raw Material Cost of Varying Designs

	0.05m Radius	0.075m Radius	0.1m Radius	0.125m Radius
4.256m Max Height	$50,331.33	$70,365.07	$98,412.31	$134,473.05
8.512m Max Height	$75,112.12	$101,150.96	$137,605.35	$184,475.27
17.024m Max Height	$131,329.57	$171,878.69	$228,647.47	$301,635.90

5.0 Conclusion

5.1 Discussion

The main goal was to find a structurally robust, aesthetic, and cost-effective design for a skylight of approximately 10 meters by 14 meters to allow for sunlight to enter a mall. The design was initially made as a two-dimensional pattern, then lifted into three dimensions. From there, there was a large amount of freedom related to scaling the height and the beam dimensions, allowing for countless designs. Twelve different designs were chosen: all combinations of three scaled heights and four differing beam radii. Through this approach, an optimal design was found.

The optimal design for the structure follows the pattern laid out in Figure 5.1. It has a maximum height of 4.256, a rod radius of 75mm, a safety factor of 25.79, and an estimated cost of $70,365.07.

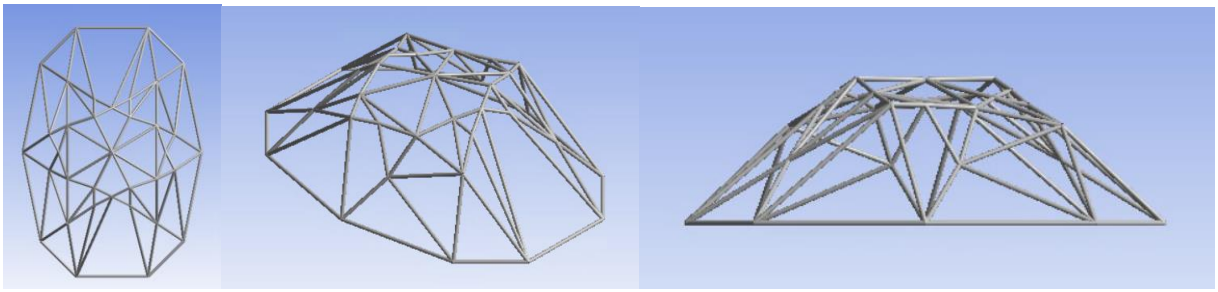

Figure 5.1: The Final Design

5.2 Future Work

There are two main routes for future work to be done on this project: generating structures and optimizing structures. Regarding the generation of structures, one problem that arose when deciding upon a pattern was the lack of certainty in a dome-like structure. In computing planar lifts, there were patterns that created concave pockets in the design. These pockets would be a large flaw in any roof design, as they will greatly accumulate rain or snow and lead to larger forces exerted on the system. An ideal path forward would be to discover what makes a planar lift concave or convex.

Regarding the optimization of structures, one path forward would be to find the absolute best design for a given pattern. This could be done by generating many more parameters for height and rod radius and creating a function to extrapolate and estimate the ideal design. My time was limited, only allowing for 12 structures, but with more varying heights and rod radii, a more ideal design may be found. Another way to work with the optimization of structures is to run similar models with load-bearing glass panes and check for any significant changes between the analyses.

Appendix

For all tables in the appendix, values are referring to either numbered points or numbered faces. Figure A1 shows the numbering system used.

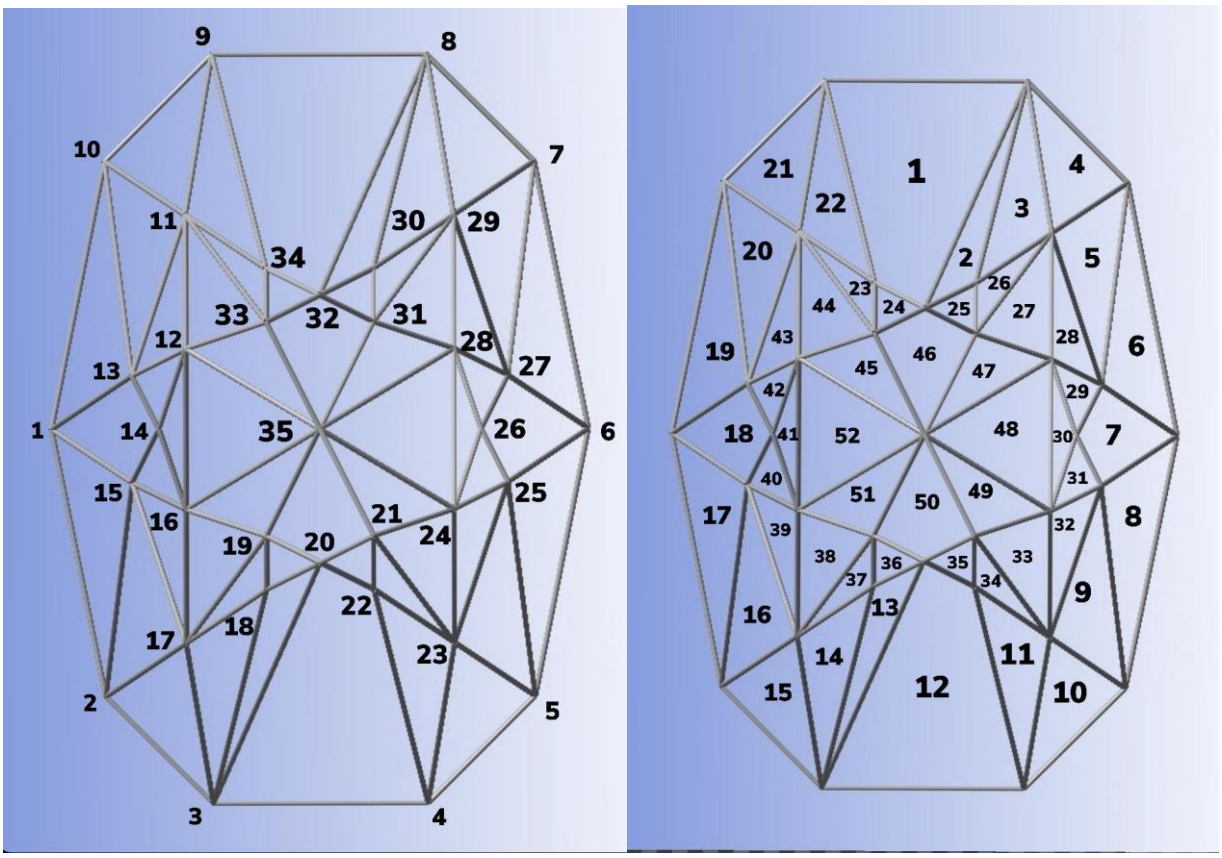

Figure A1: The Numbering of the Points (left) and Faces (right)

Table A1: Glass Panel Areas, Dead Loads, and Live Loads

	Area (m^2)			Windows Dead Load (N)			Live Load (N)		
Face	Max Height 4.256	Max Height 8.512	Max Height 17.024	Max Height 4.256	Max Height 8.512	Max Height 17.024	Max Height 4.256	Max Height 8.512	Max Height 17.024
1	14.235	21.537	38.841	7077.23	10707.57	19310.61	13637.13	20632.45	37209.68
2	2.3173	3.506	6.323	1152.09	1743.08	3143.61	2219.97	3358.75	6057.43
3	3.4341	5.3312	9.7436	1707.33	2650.52	4844.23	3289.87	5107.29	9334.37
4	4.7549	8.4668	16.371	2364.00	4209.45	8139.18	4555.19	8111.19	15683.42
5	5.615	10.17	19.774	2791.61	5056.23	9831.06	5379.17	9742.86	18943.49

6	5.45	9.334	17.799	2709.58	4640.59	8849.14	5221.10	8941.97	17051.44
7	4.3828	8.0521	15.727	2179.00	4003.27	7819.01	4198.72	7713.91	15066.47
8	9.4775	18.1	35.76	4711.94	8998.79	17778.83	9079.45	17339.80	34258.08
9	4.0056	6.4413	11.97	1991.47	3202.43	5951.13	3837.36	6170.77	11467.26
10	3.6207	5.8042	10.771	1800.11	2885.68	5355.03	3468.63	5560.42	10318.62
11	3.425	5.3077	9.6921	1702.81	2638.83	4818.63	3281.15	5084.78	9285.03
12	14.235	21.537	38.841	7077.23	10707.57	19310.61	13637.13	20632.45	37209.68
13	2.3173	3.506	6.323	1152.09	1743.08	3143.61	2219.97	3358.75	6057.43
14	3.4341	5.3312	9.7436	1707.33	2650.52	4844.23	3289.87	5107.29	9334.37
15	4.7549	8.4668	16.371	2364.00	4209.45	8139.18	4555.19	8111.19	15683.42
16	5.615	10.17	19.774	2791.61	5056.23	9831.06	5379.17	9742.86	18943.49
17	5.45	9.334	17.799	2709.58	4640.59	8849.14	5221.10	8941.97	17051.44
18	4.3828	8.0521	15.727	2179.00	4003.27	7819.01	4198.72	7713.91	15066.47
19	9.4775	18.1	35.76	4711.94	8998.79	17778.83	9079.45	17339.80	34258.08
20	4.0056	6.4413	11.97	1991.47	3202.43	5951.13	3837.36	6170.77	11467.26
21	3.6207	5.8042	10.771	1800.11	2885.68	5355.03	3468.63	5560.42	10318.62
22	3.425	5.3077	9.6921	1702.81	2638.83	4818.63	3281.15	5084.78	9285.03
23	1.0407	1.6262	2.9816	517.41	808.50	1482.36	996.99	1557.90	2856.37
24	0.63569	0.93082	1.6479	316.05	462.78	819.29	608.99	891.73	1578.69
25	0.53669	0.63416	0.92664	266.83	315.29	460.70	514.15	607.53	887.72
26	0.79224	0.90723	1.2668	393.88	451.05	629.82	758.97	869.13	1213.59
27	1.9806	2.2681	3.167	984.70	1127.63	1574.54	1897.41	2172.84	3033.99
28	2.5523	4.6227	8.9883	1268.93	2298.27	4468.72	2445.10	4428.55	8610.79
29	1.4898	2.776	5.4454	740.69	1380.15	2707.29	1427.23	2659.41	5216.69
30	0.78023	0.8646	1.1413	387.91	429.85	567.42	747.46	828.29	1093.37
31	0.65019	0.7205	0.95112	323.26	358.21	472.87	622.88	690.24	911.17
32	1.8207	2.9279	5.4408	905.20	1455.67	2705.01	1744.23	2804.93	5212.29
33	2.6016	4.0654	7.454	1293.44	2021.20	3705.91	2492.33	3894.65	7140.93
34	1.0407	1.6262	2.9816	517.41	808.50	1482.36	996.99	1557.90	2856.37
35	0.63569	0.93082	1.6479	316.05	462.78	819.29	608.99	891.73	1578.69
36	0.53669	0.63416	0.92664	266.83	315.29	460.70	514.15	607.53	887.72

37	0.79224	0.90723	1.2668	393.88	451.05	629.82	758.97	869.13	1213.59
38	1.9806	2.2681	3.167	984.70	1127.63	1574.54	1897.41	2172.84	3033.99
39	2.5523	4.6227	8.9883	1268.93	2298.27	4468.72	2445.10	4428.55	8610.79
40	1.4898	2.776	5.4454	740.69	1380.15	2707.29	1427.23	2659.41	5216.69
41	0.78023	0.8646	1.1413	387.91	429.85	567.42	747.46	828.29	1093.37
42	0.65019	0.7205	0.95112	323.26	358.21	472.87	622.88	690.24	911.17
43	1.8207	2.9279	5.4408	905.20	1455.67	2705.01	1744.23	2804.93	5212.29
44	2.6016	4.0654	7.454	1293.44	2021.20	3705.91	2492.33	3894.65	7140.93
45	1.8205	2.0174	2.6631	905.10	1002.99	1324.02	1744.04	1932.67	2551.25
46	2.62	2.9509	4.0102	1302.59	1467.10	1993.75	2509.96	2826.96	3841.77
47	1.8205	2.0174	2.6631	905.10	1002.99	1324.02	1744.04	1932.67	2551.25
48	3.9012	4.323	5.7067	1939.56	2149.27	2837.20	3737.35	4141.43	5467.02
49	1.8205	2.0174	2.6631	905.10	1002.99	1324.02	1744.04	1932.67	2551.25
50	2.62	2.9509	4.0102	1302.59	1467.10	1993.75	2509.96	2826.96	3841.77
51	1.8205	2.0174	2.6631	905.10	1002.99	1324.02	1744.04	1932.67	2551.25
52	3.9012	4.323	5.7067	1939.56	2149.27	2837.20	3737.35	4141.43	5467.02

Table A2: Wind Loads on Glass Panels

	$A_{CS,\ Horizontal\ Projection}$ (m^2)			α				Wind Load (N)		
Face	Max Height 4.256	Max Height 8.512	Max Height 17.024	Max Height 4.256	Max Height 8.512	Max Height 17.024	Wind-ward?	Max Height 4.256	Max Height 8.512	Max Height 17.024
1	0	0	0	41	60.06	73.93	Y	0.00	0.00	0.00
2	0	0	0	41	60.06	73.93	Y	0.00	0.00	0.00
3	0.512	1.024	2.048	43.28	62.03	75.1	N	2.06	5.32	11.63
4	2.86	5.72	11.44	58.28	72.83	81.22	Y	28.60	64.25	132.93
5	4.862	9.724	19.448	60.68	74.3	82.01	Y	49.84	110.06	226.43
6	4.29	8.58	17.16	53.39	69.6	79.48	Y	40.49	94.55	198.36
7	3.472	6.944	13.888	62.85	75.62	82.69	Y	36.32	79.08	161.96
8	8.73	17.46	34.92	69.95	79.7	84.79	Y	96.42	201.97	408.86
9	1.958	3.916	7.832	46.64	64.73	76.7	Y	16.74	41.64	89.61

10	1.852	3.704	7.408	46.33	64.5	76.58	Y	15.75	39.31	84.72
11	1.504	3.008	6.016	43.12	61.9	75.05	Y	12.09	31.20	68.34
12	0	0	0	41	60.06	73.93	N	0.00	0.00	0.00
13	0	0	0	41	60.06	73.93	N	0.00	0.00	0.00
14	0.512	1.024	2.048	43.28	62.03	75.1	Y	4.13	10.63	23.27
15	2.86	5.72	11.44	58.28	72.83	81.22	N	14.30	32.13	66.46
16	4.862	9.724	19.448	60.68	74.3	82.01	N	24.92	55.03	113.22
17	4.29	8.58	17.16	53.39	69.6	79.48	N	20.24	47.27	99.18
18	3.472	6.944	13.888	62.85	75.62	82.69	N	18.16	39.54	80.98
19	8.73	17.46	34.92	69.95	79.7	84.79	N	48.21	100.99	204.43
20	1.958	3.916	7.832	46.64	64.73	76.7	N	8.37	20.82	44.81
21	1.852	3.704	7.408	46.33	64.5	76.58	N	7.87	19.65	42.36
22	1.504	3.008	6.016	43.12	61.9	75.05	N	6.04	15.60	34.17
23	0.418	0.836	1.672	43.89	62.53	75.43	N	1.70	4.36	9.51
24	0	0	0	38.1	57.51	72.34	N	0.00	0.00	0.00
25	0.165	0.33	0.66	21.31	38	57.3	Y	0.70	2.39	6.53
26	0.202	0.404	0.808	18.79	34.2	53.7	Y	0.76	2.67	7.66
27	0.505	1.01	2.02	18.79	34.2	53.7	Y	1.91	6.67	19.14
28	2.21	4.42	8.84	60.7	74.31	82.01	Y	22.66	50.03	102.92
29	1.271	2.542	5.084	65.2	76.99	83.41	Y	13.57	29.12	59.38
30	0.186	0.372	0.744	16	29.84	48.92	Y	0.60	2.18	6.59
31	0.155	0.31	0.62	16	29.84	48.92	Y	0.50	1.81	5.49
32	0.89	1.78	3.56	46.63	64.73	76.7	Y	7.61	18.93	40.73
33	1.045	2.09	4.18	43.89	62.53	75.43	Y	8.52	21.80	47.56
34	0.418	0.836	1.672	43.89	62.53	75.43	Y	3.41	8.72	19.03
35	0	0	0	38.1	57.51	72.34	Y	0.00	0.00	0.00
36	0.165	0.33	0.66	21.31	38	57.3	N	0.35	1.19	3.26
37	0.202	0.404	0.808	18.79	34.2	53.7	N	0.38	1.33	3.83
38	0.505	1.01	2.02	18.79	34.2	53.7	N	0.96	3.34	9.57
39	2.21	4.42	8.84	60.7	74.31	82.01	N	11.33	25.02	51.46
40	1.271	2.542	5.084	65.2	76.99	83.41	N	6.78	14.56	29.69

41	0.186	0.372	0.744	16	29.84	48.92	N	0.30	1.09	3.30
42	0.155	0.31	0.62	16	29.84	48.92	N	0.25	0.91	2.75
43	0.89	1.78	3.56	46.63	64.73	76.7	N	3.80	9.46	20.37
44	1.045	2.09	4.18	43.89	62.53	75.43	N	4.26	10.90	23.78
45	0.434	0.868	1.736	16	29.84	48.92	N	0.70	2.54	7.69
46	0.72	1.44	2.88	17.41	32.09	51.43	Y	2.53	8.99	26.47
47	0.434	0.868	1.736	16	29.8	48.92	Y	1.41	5.07	15.39
48	0.93	1.86	3.72	16	29.8	48.92	Y	3.01	10.87	32.97
49	0.434	0.868	1.736	16	29.84	48.92	Y	1.41	5.08	15.39
50	0.72	1.44	2.88	17.41	32.09	51.43	N	1.27	4.50	13.24
51	0.434	0.868	1.736	16	29.8	48.92	N	0.70	2.54	7.69
52	0.93	1.86	3.72	16	29.8	48.92	N	1.51	5.43	16.48

Table A3: Snow Loads on Glass Panels

		Snow Load (N)		
Face	$A_{CS,\ Vertical\ Projection}$ (m^2)	Max Height 4.256 m	Max Height 8.512 m	Max Height 17.024 m
1	10.75	25735.50	25735.50	25735.50
2	1.75	4189.50	4189.50	4189.50
3	2.5	5985.00	5985.00	5985.00
4	2.5	5985.00	5985.00	5985.00
5	2.75	6583.50	6583.50	6583.50
6	3.25	7780.50	7780.50	7780.50
7	2	4788.00	4788.00	4788.00
8	3.25	7780.50	7780.50	7780.50
9	2.75	6583.50	6583.50	6583.50
10	2.5	5985.00	5985.00	5985.00
11	2.5	5985.00	5985.00	5985.00
12	10.75	25735.50	25735.50	25735.50
13	1.75	4189.50	4189.50	4189.50
14	2.5	5985.00	5985.00	5985.00

15	2.5	5985.00	5985.00	5985.00
16	2.75	6583.50	6583.50	6583.50
17	3.25	7780.50	7780.50	7780.50
18	2	4788.00	4788.00	4788.00
19	3.25	7780.50	7780.50	7780.50
20	2.75	6583.50	6583.50	6583.50
21	2.5	5985.00	5985.00	5985.00
22	2.5	5985.00	5985.00	5985.00
23	0.75	1795.50	1795.50	1795.50
24	0.5	1197.00	1197.00	1197.00
25	0.5	1197.00	1197.00	1197.00
26	0.75	1795.50	1795.50	1795.50
27	1.875	4488.75	4488.75	4488.75
28	1.25	2992.50	2992.50	2992.50
29	0.625	1496.25	1496.25	1496.25
30	0.75	1795.50	1795.50	1795.50
31	0.625	1496.25	1496.25	1496.25
32	1.25	2992.50	2992.50	2992.50
33	1.875	4488.75	4488.75	4488.75
34	0.75	1795.50	1795.50	1795.50
35	0.5	1197.00	1197.00	1197.00
36	0.5	1197.00	1197.00	1197.00
37	0.75	1795.50	1795.50	1795.50
38	1.875	4488.75	4488.75	4488.75
39	1.25	2992.50	2992.50	2992.50
40	0.625	1496.25	1496.25	1496.25
41	0.75	1795.50	1795.50	1795.50
42	0.625	1496.25	1496.25	1496.25
43	1.25	2992.50	2992.50	2992.50
44	1.875	4488.75	4488.75	4488.75
45	1.75	4189.50	4189.50	4189.50

46	2.5	5985.00	5985.00	5985.00
47	1.75	4189.50	4189.50	4189.50
48	3.75	8977.50	8977.50	8977.50
49	1.75	4189.50	4189.50	4189.50
50	2.5	5985.00	5985.00	5985.00
51	1.75	4189.50	4189.50	4189.50
52	3.75	8977.50	8977.50	8977.50

Table A4: Seismic Loads on the Glass Panels (N)

	Area (m^2)			Seismic Load (N)		
Face	Max Height 4.256 m	Max Height 8.512 m	Max Height 17.024 m	Max Height 4.256 m	Max Height 8.512 m	Max Height 17.024 m
1	14.235	21.537	38.841	129.86	196.47	354.32
2	2.3173	3.506	6.323	21.14	31.98	57.68
3	3.4341	5.3312	9.7436	31.33	48.63	88.89
4	4.7549	8.4668	16.371	43.38	77.24	149.34
5	5.615	10.17	19.774	51.22	92.77	180.39
6	5.45	9.334	17.799	49.72	85.15	162.37
7	4.3828	8.0521	15.727	39.98	73.45	143.47
8	9.4775	18.1	35.76	86.46	165.12	326.22
9	4.0056	6.4413	11.97	36.54	58.76	109.20
10	3.6207	5.8042	10.771	33.03	52.95	98.26
11	3.425	5.3077	9.6921	31.24	48.42	88.42
12	14.235	21.537	38.841	129.86	196.47	354.32
13	2.3173	3.506	6.323	21.14	31.98	57.68
14	3.4341	5.3312	9.7436	31.33	48.63	88.89
15	4.7549	8.4668	16.371	43.38	77.24	149.34
16	5.615	10.17	19.774	51.22	92.77	180.39
17	5.45	9.334	17.799	49.72	85.15	162.37
18	4.3828	8.0521	15.727	39.98	73.45	143.47

19	9.4775	18.1	35.76	86.46	165.12	326.22
20	4.0056	6.4413	11.97	36.54	58.76	109.20
21	3.6207	5.8042	10.771	33.03	52.95	98.26
22	3.425	5.3077	9.6921	31.24	48.42	88.42
23	1.0407	1.6262	2.9816	9.49	14.83	27.20
24	0.63569	0.93082	1.6479	5.80	8.49	15.03
25	0.53669	0.63416	0.92664	4.90	5.79	8.45
26	0.79224	0.90723	1.2668	7.23	8.28	11.56
27	1.9806	2.2681	3.167	18.07	20.69	28.89
28	2.5523	4.6227	8.9883	23.28	42.17	81.99
29	1.4898	2.776	5.4454	13.59	25.32	49.68
30	0.78023	0.8646	1.1413	7.12	7.89	10.41
31	0.65019	0.7205	0.95112	5.93	6.57	8.68
32	1.8207	2.9279	5.4408	16.61	26.71	49.63
33	2.6016	4.0654	7.454	23.73	37.09	68.00
34	1.0407	1.6262	2.9816	9.49	14.83	27.20
35	0.63569	0.93082	1.6479	5.80	8.49	15.03
36	0.53669	0.63416	0.92664	4.90	5.79	8.45
37	0.79224	0.90723	1.2668	7.23	8.28	11.56
38	1.9806	2.2681	3.167	18.07	20.69	28.89
39	2.5523	4.6227	8.9883	23.28	42.17	81.99
40	1.4898	2.776	5.4454	13.59	25.32	49.68
41	0.78023	0.8646	1.1413	7.12	7.89	10.41
42	0.65019	0.7205	0.95112	5.93	6.57	8.68
43	1.8207	2.9279	5.4408	16.61	26.71	49.63
44	2.6016	4.0654	7.454	23.73	37.09	68.00
45	1.8205	2.0174	2.6631	16.61	18.40	24.29
46	2.62	2.9509	4.0102	23.90	26.92	36.58
47	1.8205	2.0174	2.6631	16.61	18.40	24.29
48	3.9012	4.323	5.7067	35.59	39.44	52.06
49	1.8205	2.0174	2.6631	16.61	18.40	24.29

50	2.62	2.9509	4.0102	23.90	26.92	36.58
51	1.8205	2.0174	2.6631	16.61	18.40	24.29
52	3.9012	4.323	5.7067	35.59	39.44	52.06

Table A5: Total Glass Panel Loads (N)

	Max Height 4.256 m		**Max Height 8.512 m**		**Max Height 17.024 m**	
Face	**F_y**	**F_z**	**F_y**	**F_z**	**F_y**	**F_z**
1	-46449.86	129.86	-57075.51	196.47	-82255.79	354.32
2	-7561.57	21.14	-9291.33	31.98	-13390.54	57.68
3	-10982.20	33.39	-13742.81	53.95	-20163.60	100.52
4	-12904.19	71.98	-18305.64	141.49	-29807.60	282.27
5	-14754.28	101.06	-21382.59	202.84	-35358.05	406.82
6	-15711.18	90.20	-21363.06	179.70	-33681.09	360.73
7	-11165.72	76.30	-16505.18	152.54	-27673.47	305.42
8	-21571.88	182.88	-34119.09	367.09	-59817.41	735.08
9	-12412.33	53.28	-15956.69	100.40	-24001.89	198.81
10	-11253.74	48.78	-14431.10	92.25	-21658.64	182.98
11	-10968.96	43.33	-13708.61	79.62	-20088.66	156.75
12	-46449.86	129.86	-57075.51	196.47	-82255.79	354.32
13	-7561.57	21.14	-9291.33	31.98	-13390.54	57.68
14	-10982.20	35.45	-13742.81	59.27	-20163.60	112.15
15	-12904.19	57.68	-18305.64	109.36	-29807.60	215.81
16	-14754.28	76.14	-21382.59	147.81	-35358.05	293.60
17	-15711.18	69.96	-21363.06	132.42	-33681.09	261.55
18	-11165.72	58.14	-16505.18	113.00	-27673.47	224.45
19	-21571.88	134.67	-34119.09	266.10	-59817.41	530.65
20	-12412.33	44.91	-15956.69	79.58	-24001.89	154.00
21	-11253.74	40.90	-14431.10	72.60	-21658.64	140.62
22	-10968.96	37.29	-13708.61	64.02	-20088.66	122.58
23	-3309.90	11.20	-4161.90	19.20	-6134.24	36.71

24	-2122.04	5.80	-2551.50	8.49	-3594.98	15.03
25	-1977.98	5.60	-2119.81	8.17	-2545.42	14.98
26	-2948.34	7.99	-3115.67	10.95	-3638.91	19.21
27	-7370.86	19.98	-7789.22	27.37	-9097.28	48.03
28	-6706.53	45.94	-9719.32	92.20	-16072.01	184.92
29	-3664.16	27.16	-5535.80	54.44	-9420.24	109.05
30	-2930.87	7.72	-3053.64	10.06	-3456.29	17.01
31	-2442.39	6.43	-2544.70	8.39	-2880.29	14.17
32	-5641.93	24.22	-7253.09	45.63	-10909.79	90.37
33	-8274.52	32.25	-10404.60	58.89	-15335.59	115.56
34	-3309.90	12.90	-4161.90	23.56	-6134.24	46.23
35	-2122.04	5.80	-2551.50	8.49	-3594.98	15.03
36	-1977.98	5.25	-2119.81	6.98	-2545.42	11.72
37	-2948.34	7.61	-3115.67	9.61	-3638.91	15.38
38	-7370.86	19.02	-7789.22	24.03	-9097.28	38.46
39	-6706.53	34.61	-9719.32	67.19	-16072.01	133.46
40	-3664.16	20.37	-5535.80	39.88	-9420.24	79.36
41	-2930.87	7.42	-3053.64	8.98	-3456.29	13.71
42	-2442.39	6.18	-2544.70	7.48	-2880.29	11.42
43	-5641.93	20.41	-7253.09	36.17	-10909.79	70.00
44	-8274.52	27.99	-10404.60	47.99	-15335.59	91.78
45	-6838.64	17.31	-7125.16	20.94	-8064.77	31.99
46	-9797.55	26.43	-10279.06	35.91	-11820.53	63.06
47	-6838.64	18.01	-7125.16	23.48	-8064.77	39.68
48	-14654.41	38.60	-15268.20	50.30	-17281.72	85.03
49	-6838.64	18.01	-7125.16	23.48	-8064.77	39.68
50	-9797.55	25.17	-10279.06	31.42	-11820.53	49.82
51	-6838.64	17.31	-7125.16	20.94	-8064.77	31.99
52	-14654.41	37.10	-15268.20	44.87	-17281.72	68.54

Table A6: Element Numbers Versus Endpoints

Element Number	Endpoint A	Endpoint B
1	1	2
2	2	3
3	3	4
4	4	5
5	5	6
6	6	7
7	7	8
8	8	9
9	9	10
10	10	1
11	10	11
12	11	34
13	34	32
14	32	31
15	31	28
16	28	27
17	27	6
18	6	25
19	25	24
20	24	21
21	21	20
22	20	18
23	18	17
24	17	2
25	7	29
26	29	30
27	30	32
28	32	33
29	33	12

30	12	13
31	13	1
32	1	15
33	15	16
34	16	19
35	19	20
36	20	22
37	22	23
38	23	5
39	9	11
40	9	34
41	8	32
42	8	30
43	8	29
44	10	13
45	11	13
46	11	12
47	11	33
48	33	34
49	30	31
50	29	31
51	29	28
52	29	27
53	27	7
54	14	12
55	14	13
56	14	15
57	14	16
58	12	16
59	35	12
60	35	33

61	35	31
62	35	28
63	35	24
64	35	21
65	35	19
66	35	16
67	24	28
68	26	24
69	26	25
70	26	27
71	26	28
72	2	15
73	17	15
74	17	16
75	17	19
76	19	18
77	21	22
78	23	21
79	23	24
80	23	25
81	5	25
82	3	17
83	3	18
84	3	20
85	4	22
86	4	23

Table A7: Buckling Strength of Elements (kN)

	0.05m Radius			0.075m Radius			0.1m Radius			0.125m Radius		
Element Number	Max Height 4.256	Max Height 8.512	Max Height 17.024	Max Height 4.256	Max Height 8.512	Max Height 17.024	Max Height 4.256	Max Height 8.512	Max Height 17.024	Max Height 4.256	Max Height 8.512	Max Height 17.024
1	129	129	129	651	651	651	2058	2058	2058	5025	5025	5025
2	418	418	418	2117	2117	2117	6690	6690	6690	16332	16332	16332
3	209	209	209	1058	1058	1058	3345	3345	3345	8166	8166	8166
4	418	418	418	2117	2117	2117	6690	6690	6690	16332	16332	16332
5	129	129	129	651	651	651	2058	2058	2058	5025	5025	5025
6	129	129	129	651	651	651	2058	2058	2058	5025	5025	5025
7	418	418	418	2117	2117	2117	6690	6690	6690	16332	16332	16332
8	209	209	209	1058	1058	1058	3345	3345	3345	8166	8166	8166
9	418	418	418	2117	2117	2117	6690	6690	6690	16332	16332	16332
10	129	129	129	651	651	651	2058	2058	2058	5025	5025	5025
11	501	197	58	2535	998	291	8012	3154	921	19560	7699	2248
12	569	243	74	2883	1232	374	9110	3893	1183	22242	9504	2888
13	2325	1670	784	11773	8452	3971	37207	26713	12552	90837	65217	30644
14	2571	2300	1618	13015	11643	8191	41133	36799	25888	100422	89841	63204
15	1291	1170	849	6538	5921	4298	20663	18712	13583	50446	45684	33162
16	832	271	73	4213	1374	372	13316	4342	1175	32511	10600	2868
17	540	223	66	2733	1127	336	8639	3561	1063	21092	8694	2594
18	217	64	17	1096	325	85	3465	1029	270	8460	2511	659
19	2473	2015	1158	12521	10203	5862	39572	32247	18528	96611	78728	45235
20	1240	1017	592	6278	5149	2995	19842	16274	9465	48443	39731	23108
21	2437	1922	1042	12337	9732	5275	38992	30757	16672	95196	75090	40703
22	2325	1670	784	11773	8452	3971	37207	26713	12552	90837	65217	30644
23	923	704	362	4672	3566	1832	14765	11271	5790	36048	27517	14136
24	293	93	25	1482	471	126	4682	1488	399	11431	3633	974
25	293	93	25	1482	471	126	4682	1488	399	11431	3633	974
26	923	704	362	4672	3566	1832	14765	11271	5790	36048	27517	14136
27	2325	1670	784	11773	8452	3971	37207	26713	12552	90837	65217	30644

28	2437	1922	1042	12337	9732	5275	38992	30757	16672	95196	75090	40703
29	1240	1017	592	6278	5149	2995	19842	16274	9465	48443	39731	23108
30	2473	2015	1158	12521	10203	5862	39572	32247	18528	96611	78728	45235
31	217	64	17	1096	325	85	3465	1029	270	8460	2511	659
32	540	223	66	2733	1127	336	8639	3561	1063	21092	8694	2594
33	832	271	73	4213	1374	372	13316	4342	1175	32511	10600	2868
34	1291	1170	849	6538	5921	4298	20663	18712	13583	50446	45684	33162
35	2571	2300	1618	13015	11643	8191	41133	36799	25888	100422	89841	63204
36	2325	1670	784	11773	8452	3971	37207	26713	12552	90837	65217	30644
37	569	243	74	2883	1232	374	9110	3893	1183	22242	9504	2888
38	501	197	58	2535	998	291	8012	3154	921	19560	7699	2248
39	264	146	52	1335	737	264	4221	2330	835	10304	5688	2037
40	115	51	16	583	260	81	1842	821	255	4497	2003	623
41	85	39	12	429	199	63	1355	628	199	3307	1532	487
42	115	51	16	583	260	81	1842	821	255	4497	2003	623
43	192	80	24	972	403	121	3070	1275	382	7496	3113	932
44	118	51	16	595	260	80	1881	823	253	4593	2009	618
45	264	161	63	1334	816	319	4217	2578	1009	10296	6294	2464
46	331	155	49	1678	783	250	5303	2476	790	12947	6044	1929
47	278	114	34	1408	577	172	4449	1822	542	10862	4449	1324
48	2072	967	309	10487	4896	1563	33144	15473	4939	80919	37777	12059
49	3206	2851	1977	16231	14435	10006	51297	45622	31625	125238	111381	77210
50	483	374	197	2446	1894	996	7731	5986	3146	18874	14615	7682
51	513	456	316	2597	2310	1601	8208	7299	5060	20038	17821	12354
52	296	220	108	1497	1111	547	4732	3513	1730	11554	8576	4223
53	174	119	53	882	604	267	2788	1909	845	6807	4662	2062
54	1279	1129	769	6474	5716	3893	20461	18065	12304	49953	44105	30039
55	2675	2672	2662	13542	13529	13477	42800	42759	42595	104492	104391	103993
56	772	246	66	3907	1247	335	12349	3940	1058	30150	9618	2583
57	1333	1320	1269	6750	6683	6425	21335	21121	20307	52086	51564	49577
58	364	343	279	1843	1737	1413	5826	5491	4465	14222	13405	10901

59	386	365	301	1955	1850	1524	6177	5847	4816	15082	14275	11759
60	669	668	666	3386	3382	3369	10700	10690	10649	26123	26098	25998
61	633	544	349	3203	2754	1764	10122	8703	5577	24711	21248	13615
62	364	296	170	1841	1499	860	5818	4738	2719	14203	11567	6638
63	386	365	301	1955	1850	1524	6177	5847	4816	15082	14275	11759
64	669	668	666	3386	3382	3369	10700	10690	10649	26123	26098	25998
65	633	544	349	3203	2754	1764	10122	8703	5577	24711	21248	13615
66	364	296	170	1841	1499	860	5818	4738	2719	14203	11567	6638
67	364	343	279	1843	1737	1413	5826	5491	4465	14222	13405	10901
68	1279	1129	769	6474	5716	3893	20461	18065	12304	49953	44105	30039
69	2675	2672	2662	13542	13529	13477	42800	42759	42595	104492	104391	103993
70	772	246	66	3907	1247	335	12349	3940	1058	30150	9618	2583
71	1333	1320	1269	6750	6683	6425	21335	21121	20307	52086	51564	49577
72	174	119	53	882	604	267	2788	1909	845	6807	4662	2062
73	296	220	108	1497	1111	547	4732	3513	1730	11554	8576	4223
74	513	456	316	2597	2310	1601	8208	7299	5060	20038	17821	12354
75	483	374	197	2446	1894	996	7731	5986	3146	18874	14615	7682
76	3206	2851	1977	16231	14435	10006	51297	45622	31625	125238	111381	77210
77	2072	967	309	10487	4896	1563	33144	15473	4939	80919	37777	12059
78	278	114	34	1408	577	172	4449	1822	542	10862	4449	1324
79	331	155	49	1678	783	250	5303	2476	790	12947	6044	1929
80	264	161	63	1334	816	319	4217	2578	1009	10296	6294	2464
81	118	51	16	595	260	80	1881	823	253	4593	2009	618
82	192	80	24	972	403	121	3070	1275	382	7496	3113	932
83	115	51	16	583	260	81	1842	821	255	4497	2003	623
84	85	39	12	429	199	63	1355	628	199	3307	1532	487
85	115	51	16	583	260	81	1842	821	255	4497	2003	623
86	264	146	52	1335	737	264	4221	2330	835	10304	5688	2037

References

[1] Baker, W. (Feb. 2021). Maximizing the Number of Planar Lifts (and why structural engineers care). Fields Institute for Research in Mathematical Sciences. url: http://www.fields.utoronto.ca/talks/Maximizing-Number-Planar-Lifts-and-why-structural-engineers-care.

[2] Leonard, S., Quinn, G. (2022). *3D Liftings and Edge-Crossing Replacements of Quad-Dominated Frameworks.* Tech. rep. Worcester Polytechnic Institute.

[3] Scholz, A. (2003). *3D Liftings of over braced rigid planar frameworks from the generic 2-rigidity matroid.* Tech. rep. Worcester Polytechnic Institute.

[4] *Ansys® Academic Research Mechanical, Release 18.1*

[5] Liu, Changyu, et al. "Influence of PCM Design Parameters on Thermal and Optical Performance of Multi-Layer Glazed Roof." *Applied Energy*, Elsevier, 8 Dec. 2017, www.sciencedirect.com/science/article/pii/S0306261917317257.

[6] Board of Building Regulations and Standards. "MA State Building Code, 9th Ed, Base Volume." *UpCodes*, up.codes/viewer/massachusetts/ibc-2015/chapter/16/structural-design#16.

[7] U.S. Department of Housing and Urban Development. "Chapter 3: Design Loads for Residential Buildings - HUD USER." *HUD User*, www.huduser.gov/Publications/pdf/res2000_2.pdf.

[8] *780 CMR: State Board of Building Regulations and Standards - Massachusetts*. Board of Building Regulations and Standards, www.mass.gov/doc/780016pt4pdf/download.

[9] Tietsma, Gerard J. "Getting the Edge on Roof Wind Design." *International Institute of Building Closure Consultants (IBEC)*, Apr. 2003, iibec.org/wp-content/uploads/2016/04/2003-04-teitsma.pdf.

[10] "Kite Inclination Effects on Lift and Drag." *NASA*, NASA, www.grc.nasa.gov/WWW/k-12/airplane/kiteincl.html#:~:text=For%20a%20thin%20flat%20plate%20at%20a%20low,trigonometric%20sine%2C%20sin%2C%20of%20the%20angle%20a%20%3A.

[11] Szyk, Bogna. "Snow Load Calculator." *Weight of Snow on Your Roof*, Omni Calculator, 6 Apr. 2022, www.omnicalculator.com/construction/snow-load.

[12] "Roof Snow Load Calculator." *Inch Calculator*, 25 Aug. 2021, www.inchcalculator.com/roof-snow-load-calculator/.

[13] “Seismic Design Requirements, H-18-8.” *National Earthquake Hazards Reduction Provisions*, U.S. Department of Veterans Affairs, www.nehrp.gov/pdf/H-18-8.pdf.

[14] “Design of Aluminum Structure.” *CE-REF*, ce-ref.com/Alumnium_design/Alum_tension/Aluminum_tension.html.

[15]“Relevant Codes & Standards for Aluminum Walkway Covers.” *Mitchell Metals*, 16 May 2019, www.mitchellmetals.net/for-architects/engineering/ibc-asce-codes/#:~:text=%28This%20sections%20deals%20specifically%20with%20allowable%20deflection%20for,the%20total%20load%20deflection%20shall%20not%20exceed%20L%2F60.

[16] “Metal Spot Price Charts.” *Daily Metal Price*, www.dailymetalprice.com/metalpricecharts.php?c=al&u=lb&d=240.

[17] Gibson, Craig. “2022 How Much Does Glass and Glazing Cost?” *Hipages*, 24 Mar. 2022, hipages.com.au/article/how_much_does_glass_and_glazing_cost.